

In-situ growth of superconducting MgB₂ thin films by molecular beam epitaxy

K Ueda*, M. Naito

NTT Basic Research Laboratories, NTT Corporation,
3-1 Wakamiya, Morinosato, Atsugi, Kanagawa 243-0198, Japan

Abstract

The in-situ growth of superconducting MgB₂ thin films was examined from various perspectives. The paper discusses (1) growth temperature, (2) the effect of excess Mg, (3) the effect of residual gas during growth, (4) the effect of in-situ annealing, (5) thickness dependence and (6) the effect of substrates. Our results provide a guide to the preparation of high-quality superconducting MgB₂ films for potential electronics applications.

PACS No.: 74.76.Db, 74.70.Ad, 74.40.-b, 73.61.At

Keywords: MgB₂, MBE, superconducting, film, in-situ annealing, gas, substrate effect, thickness dependence

1. Introduction

The discovery of superconductivity at 39 K in MgB_2 [1] has generated great scientific and technological interest. MgB_2 has many properties that make it very attractive for superconducting electronics. Unlike high- T_c cuprates, MgB_2 may be suitable, despite its lower T_c , for fabricating good Josephson junctions. This is because it has less anisotropy, fewer material complexities, fewer interface problems, and a longer coherence length ($\xi \sim 5$ nm). The reliable fabrication of Josephson junctions requires high-quality thin films of MgB_2 . In this article, we report our in-situ growth of MgB_2 films by coevaporation.

There have already been many reports on the synthesis of superconducting MgB_2 films [2-14]. There are two complicating problems related to the preparation of superconducting MgB_2 films. These are the high sensitivity of Mg to oxidation and the high Mg vapor pressure required for the thermodynamic stability of the superconducting MgB_2 phase. The former problem can be avoided by depositing MgB_2 films either in an ultra-high vacuum or in a reducing atmosphere containing hydrogen. The latter problem is more serious, and there are two ways to overcome it. One is two-step synthesis, in which amorphous B (or Mg-B composite) precursors are *ex-situ* annealed at high temperatures with high Mg vapor pressure usually in a confined container [2-6]. This two-step process produces good crystalline films with good superconducting properties although it may not be favorable for multilayer device fabrication. The other is *in-situ* (as-grown) synthesis, in which films are grown *in-situ* at low temperatures of around 300°C at the relatively low Mg vapor pressure ($10^{-5} \sim 10^{-6}$ Torr) that is compatible with many vacuum deposition techniques. *In-situ* synthesis makes multilayer deposition feasible although in most cases it only produces poor crystalline films with a T_c of ~ 35 K, which is slightly below the bulk value [10-13]. This is because good epitaxial growth is impeded due to the limited growth temperatures below $\sim 300^\circ\text{C}$. By employing a special combination of physical and chemical vapor deposition techniques, Zeng *et al.* have very recently achieved the *in-situ* epitaxial growth of MgB_2 films at around 750°C at a high Mg vapor pressure (10-100 mTorr) [14]. However, it remains to be seen whether this method is as suitable for multilayer deposition as conventional physical vapor deposition.

In the last 18 months since the discovery of MgB_2 , we have performed a fairly comprehensive survey of the parameters in *in-situ* MgB_2 film growth by coevaporation. In this article, we report the results of this survey. The following issues will be discussed [10].

- (1) Growth temperature
- (2) Effect of excess Mg
- (3) Effect of residual gas during growth
- (4) Effect of in-situ annealing
- (5) Thickness dependence
- (6) Effect of substrates

2. Experimental

We grew MgB_2 thin films in a customer-designed MBE chamber (basal pressure $< 10^{-9}$ Torr) from pure metal sources using multiple electron guns [15, 16]. The evaporation beam flux of each element was controlled by electron impact emission spectrometry (EIES) via feedback loops to the electron guns. The flux ratio of Mg to

B was changed so that it was from 1 to 10 times as high as the nominal ratio. The growth rate was 1.5 - 2 Å/s, and the film thickness was 1000 Å for typical films. We used sapphire C, sapphire R, H-terminated Si (111), SrTiO₃ (100), and glass substrates (Corning #7059).

We characterized the structure and crystallinity by X-ray diffraction (XRD, $2\theta - \theta$ scan) and reflection high-energy electron diffraction (RHEED). We measured resistivity by the standard four-probe method using electrodes formed by Ag evaporation. The composition was determined by inductively coupled plasma (ICP) spectrometric analysis. We sometimes found that ICP analysis underestimated the B content of the films perhaps due to the low solubility of B in usual acids. These questionable data were not included in the results described below.

3. Results and Discussion

3.1 Growth temperature

A very high Mg vapor pressure is required when depositing MgB₂ films at elevated temperatures. In other words, the growth temperature when depositing MgB₂ films has to be low at a low Mg vapor pressure. This conclusion can be reached both from the thermodynamic stability of the MgB₂ phase and from the growth kinetics. Given an Mg vapor pressure of 10⁻⁴ Torr, which is the upper limit compatible with vacuum evaporation techniques, the thermodynamic calculation for the Mg-B binary phase diagram reported by Liu et al [17], as shown in Fig. 1, predicts that the superconducting MgB₂ phase will decompose above 535°C. On the other hand, the growth kinetics on a substrate or film surface predicts that non-bonding Mg re-evaporates from the surface for a growth temperature above ~ 300°C in 10⁻⁴ Torr of Mg vapor according to the equilibrium Mg vapor pressure curve [18]. Both predictions suggest that the upper limit of the substrate temperature for MgB₂ growth by coevaporation will be 300 ~ 400°C.

Consistent with these considerations, we actually observed a significant Mg loss in films grown above a substrate temperature (T_s) of 300°C. Figure 2(a) shows the molar ratio of Mg to B₂ evaluated by ICP analysis in films grown at temperatures of 200°C to 500°C and also with Mg rates 1.3 to 10 times the nominal rate. The films grown above 300°C were significantly deficient in Mg even with a 10 times higher Mg rate. These Mg deficient films were transparent and insulating. This indicates that the growth temperature limit is 300°C for the in-situ growth of superconducting MgB₂ films by coevaporation. However, a slight and uncontrollable change (5°C) in the growth temperature near $T_s = 300^\circ\text{C}$ leads to a dramatic change in composition, and makes the results irreproducible. We have therefore chosen the following as our typical growth conditions: $T_s = 280^\circ\text{C}$ with an Mg rate maintained at three times the nominal rate. The resultant as-grown films on sapphire C substrates typically exhibited XRD patterns and ρ -T curves as shown in Fig. 3. The films had a c-axis preferred orientation, and their T_c and resistivity were 32 - 35 K and 30 - 50 $\mu\Omega\text{cm}$ at 300 K, respectively, which should be compared with the bulk single crystal values of 39 K and 5-10 $\mu\Omega\text{cm}$.

When the growth temperature is lowered, the crystallinity becomes poor judging from the XRD peak intensities, and simultaneously the superconducting properties become degraded as shown in Fig. 2(b). This figure shows the superconducting transition temperature of MgB₂ films grown at different T_s values on sapphire C with an Mg rate of twice the nominal rate. The T_c value decreases monotonically as T_s decreases as long as the MgB₂ phase is formed, and disappears below ~150°C. This T_c suppression is not only due to poorer crystallinity but

also due to excess Mg as described below.

3.2 Effect of excess Mg

Figure 4 shows the superconducting properties of MgB_2 films grown on sapphire C at a fixed substrate temperature (280°C) but with different Mg rates (1 ~ 10 times). The desired phase is not formed with Mg rates of less than 3 times the nominal rate. At higher Mg rates, T_c gradually decreases and eventually becomes around 15 K at 10 times the nominal Mg rate. A reduction in resistivity accompanies this T_c suppression, indicating the presence of metal Mg in these films. This result demonstrates the harmful effect of excess Mg on the superconducting properties, which is either due to the proximity effect with normal Mg metal or the formation of nonstoichiometric $\text{Mg}_{1+x}\text{B}_2$ that is hitherto unknown to be formed in bulk synthesis.

3.3 Effect of residual gas during growth

In our early attempts to grow MgB_2 , we had some difficulty in obtaining reproducible results. For example, the resistivity of Fig. 4(b) is considerably higher than the typical value in Fig. 3(b). These irreproducible results can be partly explained by the fact that the sticking coefficient of Mg varies dramatically near $T_s \sim 300^\circ\text{C}$. However, we have noticed another reason for the irreproducibility, namely the effect of residual oxygen on MgB_2 film growth. In fact, we obtained the high-resistivity film shown in Fig. 4(b) when we had a tiny leak in our MBE chamber, which gave an oxygen partial pressure of $P_{\text{O}_2} \sim 4 \times 10^{-9}$ Torr. Based on this experience, we undertook a systematic investigation of the effect of residual gas on the growth of MgB_2 films. We studied the effects of hydrogen and nitrogen in addition to that of oxygen. In this experiment, molecular O_2 , H_2 or N_2 gas was introduced into the chamber during growth. We varied the gas pressure from 3×10^{-9} to 8×10^{-6} Torr.

First, we describe the effect of oxygen on MgB_2 growth. Figure 5 shows the XRD patterns and r - T curves of MgB_2 films grown on sapphire C under two different partial oxygen pressures. Weak but definite MgB_2 (00 l) peaks are observed for the film grown in $P_{\text{O}_2} < 1.0 \times 10^{-10}$ Torr whereas no peak is observed for the film grown in $P_{\text{O}_2} \sim 3.7 \times 10^{-9}$ Torr. The resistivity of the latter film is much higher although T_c is not greatly suppressed (only ~ 3 K). For $P_{\text{O}_2} > 10^{-7}$ Torr, the films were transparent and insulating, indicating that no MgB_2 phase was formed. These observations strongly indicate that residual oxygen is very harmful to MgB_2 film growth, even with P_{O_2} as low as 1×10^{-9} Torr. This result can be readily understood from the high sensitivity of Mg to oxidation.

In contrast to oxygen, residual hydrogen and nitrogen have a negligible or even a slightly favorable effect on MgB_2 film growth. Figure 6 shows superconducting transitions of MgB_2 films grown on sapphire C in H_2 or N_2 gas with different partial pressures. The introduction of H_2 and N_2 gas even improved T_c by about 1 K. The maximum T_c improvement (~ 1.5 K) was achieved by the introduction of N_2 gas at 3.8×10^{-6} Torr. The significant resistivity increase with a hydrogen partial pressure of 5×10^{-6} Torr could be due to the fact that our hydrogen gas was less pure than the nitrogen gas. Figure 7 shows a plot of the superconducting transition temperature as a function of P_{H_2} or P_{N_2} . When N_2 gas was introduced, T_c was at its maximum around $P_{\text{N}_2} \sim 4 \times 10^{-6}$ Torr. We repeated the experiment to confirm that this effect really exists rather than being the results of scattering, and also obtained a similar trend in the second round (N_2 -2).

The origin of the slight improvement in T_c with residual H_2 or N_2 is unclear. It is conceivable, however, that

hydrogen may prevent Mg from oxidation. With nitrogen, the origin may be more complicated. One hint is provided by the fact that film crystallinity is somewhat improved by the introduction of nitrogen as shown in Fig. 8. This improved crystallinity is seemingly reflected in the lower resistivity of these films. Nitrogen may play a catalytic role in promoting the chemical reaction ($\text{Mg} + 2\text{B} \rightarrow \text{MgB}_2$) and crystallization. In this connection, it should be noted that Lee et al. have succeeded in growing MgB_2 single crystals in the Mg-B-N ternary system [19].

3.4 Effect of in-situ annealing

As seen from the above results, the properties of as-grown films are inferior to those of bulk single crystals or *ex-situ* post-annealed films in that the superconducting transition temperature is lower, namely $T_c(\text{end})$ is ~ 35 K at its highest, and the resistivity has a higher value and a weaker temperature dependence. With the aim of improving the superconducting properties of MgB_2 films, we attempted in-situ post-annealing for as-grown films. The in-situ post-annealing was performed just after growth at annealing temperatures (T_a) of $380 \sim 680^\circ\text{C}$ for 10 minutes while exposing the films to Mg flux ($\sim 4.5 \text{ \AA}/\text{sec}$). From the thermodynamic viewpoint, our recipe of the in-situ post-annealing may be outside the stability field of the MgB_2 phase as shown below. However, the very slow kinetics of the decomposition process predicts that the inside of the films will be protected from decomposition (see Fig. 1) [18]. In fact, the in-situ post-annealing slightly improved the inside of the films. Figure 9 provides a summary of the results. The XRD results suggest that annealing at T_a below 503°C did not improve the crystallinity of the films whereas annealing at $T_a = 526^\circ\text{C}$ increased the peak intensities significantly (Fig. 9(a)). The RHEED observations made during annealing indicated that the surface of the films had already started to decompose at $T_a \sim 500^\circ\text{C}$. The RHEED patterns became halo-like with annealing at $T_a \sim 550^\circ\text{C}$, above which the inside of the films also started to decompose. This situation did not change greatly even when the Mg flux rate was tripled to $\sim 15.0 \text{ \AA}/\text{sec}$.

For T_a below 503°C , although there was no improvement in the crystallinity as mentioned above, the superconducting transition temperature increased gradually with increasing T_a , and a maximum improvement of ~ 2 K was achieved by annealing at $T_a = 503^\circ\text{C}$. The resistivity was also improved although there was some scattering in the data. This improved superconductivity may result from a partial elimination of an unfavorable feature in the grain boundaries. The T_c of the film annealed at $T_a = 526^\circ\text{C}$ was slightly lower than that of the film annealed at $T_a = 503^\circ\text{C}$ in spite of its better crystallinity.

Fig. 10 compares AFM images ($1 \mu\text{m} \times 1 \mu\text{m}$ view) of the as-grown and in-situ post-annealed films. The grain size was almost the same in the as-grown films and the in-situ annealed films at 480°C ($200 - 400 \text{ \AA}$), namely in-situ annealing at 480°C does not increase the grain size. However, the grain size is slightly larger in the films annealed at 526°C . These AFM results seem to be consistent with the above XRD results (Fig. 9(a)).

The surfaces of all the films were fairly smooth, and the root-mean-square roughness (R_{MS}) and the average roughness (R_a) were 22.3 \AA and 17.7 \AA for the as-grown films, 17.4 \AA and 13.7 \AA for the post-annealed films at 480°C , and 29.6 \AA and 23.1 \AA for the post-annealed films at 526°C , respectively. The R_{MS} and R_a of the film post-annealed at 526°C were the largest reflecting the increase in the grain size.

3.5 Thickness dependence

The thickness dependence of the superconductivity was examined for both of as-grown and post-annealed films. We undertook this investigation specifically for the purpose of evaluating the degraded surface thickness of post-annealed films. The film thickness, which was controlled by changing the deposition time, was varied from 25 to 1000 Å. In this experiment, post-annealed films were prepared at $T_a = 480^\circ\text{C}$. The thickness dependences of the r - T curves are shown for as-grown films in Fig. 11, and for post-annealed films in Fig. 12. In both cases, T_c decreased and the resistivity increased with decreasing film thickness. Figure 13 is a plot of T_c as a function of film thickness. For film thicknesses greater than 100 Å, the T_c of the post-annealed films is higher than that of the as-grown films, but the situation is reversed at 50 Å. As-grown film, even with a thickness of 50 Å, is superconducting with a $T_c(\text{end})$ of ~ 10 K whereas the post-annealed film with a thickness of 50 Å is insulating. Figure 14 compares the RHEED patterns of the as-grown and post-annealed 50 Å films. The spotty patterns were changed to halo patterns by annealing [20]. These observations indicate surface decomposition due to Mg loss from the surface, which implies that our in-situ post-annealing conditions even with $T_a = 480^\circ\text{C}$ are out of the thermodynamic stability of the MgB_2 phase. Our recent tunneling experiments support this conclusion: post-annealed films have a dead surface (nonsuperconducting) layer and are unsuitable for fabricating junctions [21].

3.6 Effect of substrates

Finally we describe the effect of the substrates. Since our as-grown films are not highly crystalline, the epitaxial effect of the substrates is rather unimportant as compared with high- T_c cuprate films, in which the substrates play a significant role in improving the film quality [22]. However, we observed that MgB_2 films have a weak but finite substrate dependence. Figure 15 shows the superconducting transitions of MgB_2 films on different substrates: (a) as-grown and (b) post-annealed at $T_a = 480^\circ\text{C}$. In the as-grown films, T_c^{zero} was 32.2, 33.2, 30.3 and 29.5 K for Si (111), sapphire C, sapphire R and SrTiO_3 (100), respectively. With the post-annealed films, T_c^{zero} was 36.8, 36.6, 36.1 and 35.7 K for Si (111), sapphire C, sapphire R and SrTiO_3 (100), respectively. In both the as-grown and post-annealed films, T_c^{zero} was slightly higher on Si (111) and sapphire C than on sapphire R and SrTiO_3 (100). Si (111) and sapphire C have a hexagonal surface whereas sapphire R and SrTiO_3 (100) have a square or rectangular surface. MgB_2 has a hexagonal crystal structure with hexagonal Mg and B planes stacked alternately along the c axis [1]. Therefore it is understandable that substrates with a hexagonal surface provide slightly better results.

We also prepared MgB_2 films on glass substrates (Corning #7059). The XRD pattern and the r - T curve of the film grown at $T_s = 280^\circ\text{C}$ are shown in Fig. 16. The film showed a T_c^{zero} of 33.4 K although no distinct peaks were observed in the XRD pattern. The RHEED pattern contains rings in addition to the spots that are commonly observed on crystalline substrates. This result demonstrates that fair quality MgB_2 films can be grown even on amorphous substrates such as glass.

4. Summary

We examined various aspects of the in-situ growth of superconducting MgB_2 thin films. The following

summarizes each subsection of this article.

(1) Growth temperature: The growth temperature for depositing MgB_2 films has to be low ($\sim 300^\circ\text{C}$) at a low Mg vapor pressure ($\sim 10^{-6}$ Torr). This conclusion can be reached both from the thermodynamics of the stability of the MgB_2 phase and also from the growth kinetics.

(2) Effect of excess Mg: Excess Mg is harmful to the superconducting properties of MgB_2 due either to the proximity effect with normal Mg metal or to the formation of nonstoichiometric $\text{Mg}_{1+x}\text{B}_2$.

(3) Effect of residual gas during growth: Residual oxygen is very harmful to the film growth of MgB_2 even with a P_{O_2} of as low as 1×10^{-9} Torr. Residual hydrogen and nitrogen have a negligible or even a slightly favorable effect on MgB_2 film growth. The introduction of H_2 and N_2 gas improved T_c by about 1 K although the origin of this slight improvement is unclear.

(4) Effect of in-situ annealing: The T_c increased with increasing annealing temperature. The maximum improvement of ~ 2 K was achieved by annealing at 503°C . XRD and AFM measurements suggest that this improvement in superconductivity may result from the partial elimination of an unfavorable feature in the grain boundaries.

(5) Thickness dependence: T_c decreased and the resistivity increased with decreasing film thickness in both as-grown and in-situ annealed films. A comparison of the physical properties of as-grown and in-situ annealed films showed that the latter have a dead surface (nonsuperconducting) layer and are unsuitable for fabricating junctions.

(6) Effect of substrates: A weak but finite substrate effect was observed. A hexagonal surface slightly improves the quality of the MgB_2 film.

These results provide much information related to the preparation of high quality superconducting MgB_2 films for such applications as Josephson junctions, superconducting wire, and coated conductor.

Acknowledgements

The authors thank Dr. S. Karimoto, and Dr. H. Yamamoto for fruitful discussions, Mr. N. Honma for ICP analysis, and Dr. H. Takayanagi and Dr. S. Ishihara for their support and encouragement throughout the course of this study.

References

- [1] J. Nagamatsu, N. Nakagawa, T. Muranaka, Y. Zenitani and J. Akimitsu, *Nature* 410 (2000) 63.
- [2] W. N. Kang, Hyeong-Jin Kim, Eun-Mi Choi, C. U. Jung, and Sung-Ik Lee, *Science* 292 (2001) 1521.
- [3] C. B. Eom, M. K. Lee, J. H. Choi, L. J. Belenky, X. Song, L. D. Colley, M. T. Naus, S. Patnaik, J. Jiang, M. Rikel, A. Polyanskii, A. Gurevich, X. Y. Cai, S. D. Bu, S. E. Babcock, E. E. Hellstrom, D. C. Larbalestier, N. Rogado, K. A. Regan, M. A. Hayward, T. He, J. S. Slusky, K. Inumaru, M. K. Hass, and R. J. Cava, *Nature* 411 (2001) 558.
- [4] M. Paranthaman, C. Cantoni, H. Y. Zhai, H. M. Christen, T. Aytug, S. Sathyamurthy, E. D. Specht, J. R. Thompson, D. H. Lowndes, H. R. Kerchner, and D. K. Christen, *Appl. Phys. Lett.* 78 (2001) 3669.
- [5] S. H. Moon, J. H. Yun, H. N. Lee, J. I. Kye, H. G. Kim, W. Chung and B. Oh, *Appl. Phys. Lett.* 79 (2001) 2429.
- [6] H. Y. Zhai, H. M. Christen, L. Zhang, M. Paranthaman, C. Cantoni, B. C. Sales, P. H. Fleming, D. K. Christen, and D. H. Lowndes, *J. Mater. Res.* 16 (2001) 2759.
- [7] X. H. Zeng, A. Sukiasyan, X. X. Xi, Y. F. Hu, E. Wertz, W. Tian, H. P. Sun, X. Q. Pan, J. Lettieri, D. G. Schlom, C. O. Brubaker, Zi-Kui Liu and Qiang Li, *Appl. Phys. Lett.* 79 (2001) 1840.
- [8] H. M. Christen, H. Y. Zhai, C. Cantoni, M. Paranthaman, B. C. Sales, C. Rouleau, D. P. Norton, D. K. Christen and D. H. Lowndes, *Physica C* 353 (2001) 157.
- [9] D. H. A. Blank, H. Hilgenkamp, A. Brinkman, D. Mijatovic, G. Rijnders and H. Rogalla, *Appl. Phys. Lett.* 79 (2001) 394.
- [10] We have provided preliminary results in previous articles: K. Ueda and M. Naito, *Appl. Phys. Lett.* 79 (2001) 2046.
- [11] A. Saito, A. Kawakami, H. Shimakage and Z. Wang, *Jpn. J. Appl. Phys.*, 41 (2002) L127.
- [12] G. Grassano, W. Ramadan, V. Ferrando, E. Bellingeri, D. Marre, C. Ferdeghini, G. Grassano, M. Putti, A. S. Siri, P. Manfrinetti, A. Palenzona and A. Chincarini, *Supercond. Sci. and Tech.*, 14 (2001) 762, cond-mat/0103572.
- [13] W. Jo, J. -U. Huh, T. Ohnishi, A. F. Marshall, M. R. Beasley and R. H. Hammond, *Appl. Phys. Lett.*, 80 (2002) 3563.
- [14] X. H. Zeng, A. V. Pogrebnyakov, A. Kotcharov, J. E. Jones, X. X. Xi, E. M. Lysczek, J. M. Redwing, S. Y. Xu, Qi Li, J. Lettieri, D. G. Schlom, W. Tian, X. Q. Pan, and Z. K. Liu, *Nature Materials* 1 (2002) 35.
- [15] M. Naito, H. Sato, and H. Yamamoto, *Physica C* 293 (1997) 36.
- [16] M. Naito, H. Yamamoto, and H. Sato, *Physica C* 305 (1998) 233.
- [17] Zi-Kui Liu, D. G. Schlom, Qi Li and X. X. Xi, *Appl. Phys. Lett.*, 78 (2001) 3678.
- [18] Z. Y. Fan, D. G. Hinks, N. Newman, and J. M. Rowell, *Appl. Phys. Lett.*, 79 (2001) 87.
- [19] S. Lee, H. Mori, T. Masui, Yu. Eltsev, A. Yamamoto and S. Tajima, *J. Phys. Soc. Jpn.* 70 (2001). 2255.
- [20] Such a dramatic change in the RHEED patterns was not observed for 1000 Å films annealed at $T_a = 480^\circ\text{C}$.
- [21] K. Ueda, and M. Naito, submitted to *IEEE Trans. Appl. Superconductivity*.
- [22] H. Sato, and M. Naito, *Physica C*, 274 (1997) 221.

Figure captions

Fig. 1: (A) Mg vapor pressure curve, (B) thermodynamic phase stability line of MgB_2 (from ref. 17), and (C) kinetically limited phase stability line of MgB_2 (from ref. 18). The dotted line (10^{-4} Torr) is an upper limit of Mg vapor pressure compatible to physical vapor deposition.

Fig. 2: (a) Molar ratio of Mg to B_2 evaluated by ICP analysis in films grown at temperatures of 200°C to 500°C and also with Mg flux rates 1.3 to 10 times the nominal rate. (b) The superconducting transition temperature (T_c) of MgB_2 films grown at different substrate temperatures (T_s) on sapphire C with an Mg rate twice the nominal rate.

Fig. 3: (a) XRD pattern and (b) ρ -T curve of a typical as-grown MgB_2 film prepared on a sapphire C substrate. Peaks labeled “sub.” correspond to substrate peaks in the XRD pattern. The inset in Fig. 3 (a) and 3 (b) shows a RHEED pattern and an enlarged view of the superconducting transitions for the film, respectively.

Fig. 4: (a) T_c versus Mg flux ratio and (b) ρ -T curves of MgB_2 films prepared with different Mg fluxes at a fixed substrate temperature (280°C).

Fig. 5: (a) XRD patterns and (b) ρ -T curves of MgB_2 films prepared in various O_2 pressures. The inset in figure (b) is an enlarged view of the superconducting transitions.

Fig. 6: Superconducting transitions of MgB_2 films prepared in various (a) H_2 and (b) N_2 pressures.

Fig. 7: N_2 and H_2 pressure dependence of T_c of MgB_2 films. “ N_2 -1” and “ N_2 -2” indicate two different rounds of films prepared in various N_2 pressures.

Fig. 8: XRD patterns of MgB_2 films prepared in various N_2 pressures.

Fig. 9: (a) XRD patterns and (b) superconducting transitions of MgB_2 films annealed at various temperatures (380 ~ 526°C). The results of as-grown films are shown for comparison.

Fig. 10: AFM images (1 mm×1 mm) of an as-grown film (a) and post-annealed films at 480°C (b) and 526°C (c).

Fig. 11: (a) ρ -T curves of as-grown films with various thicknesses (50-1000 Å) and (b) an enlargement view of the superconducting transitions.

Fig. 12: (a) ρ -T curves of post-annealed films (480°C for 10 min.) with various thicknesses (100-1000 Å) and

(b) an enlargement view of the superconducting transitions.

Fig. 13: Thickness dependence of T_c of as-grown and post-annealed films.

Fig. 14: RHEED patterns of the films with thickness of 50Å (a) before (as-grown) and (b) after post-annealing at 480°C for 10 minutes.

Fig. 15: Resistivity-versus-temperature curves of (a) as-grown and (b) post-annealed films (480°C for 10 min) around T_c prepared on various substrates (Si (111) (filled circles), sapphire C (open circles), sapphire R (open squares), SrTiO_3 (100) (open diamonds)).

Fig. 16: XRD pattern (a) and ρ -T curve (b) of the MgB_2 film prepared on a glass substrate (Corning #7059). The inset in (b) is an enlarged view of the superconducting transition.

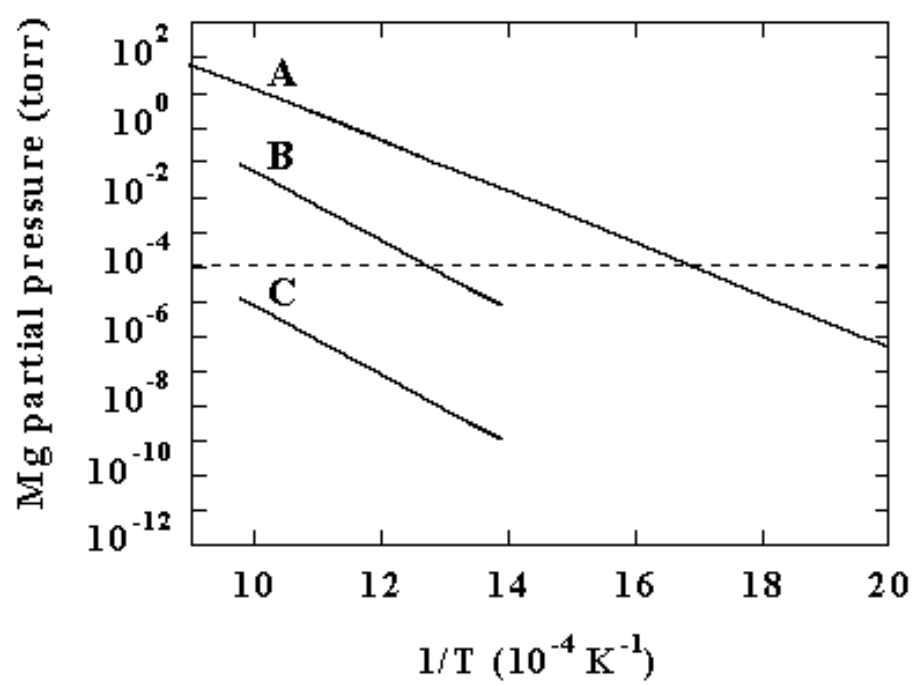


Fig. 1

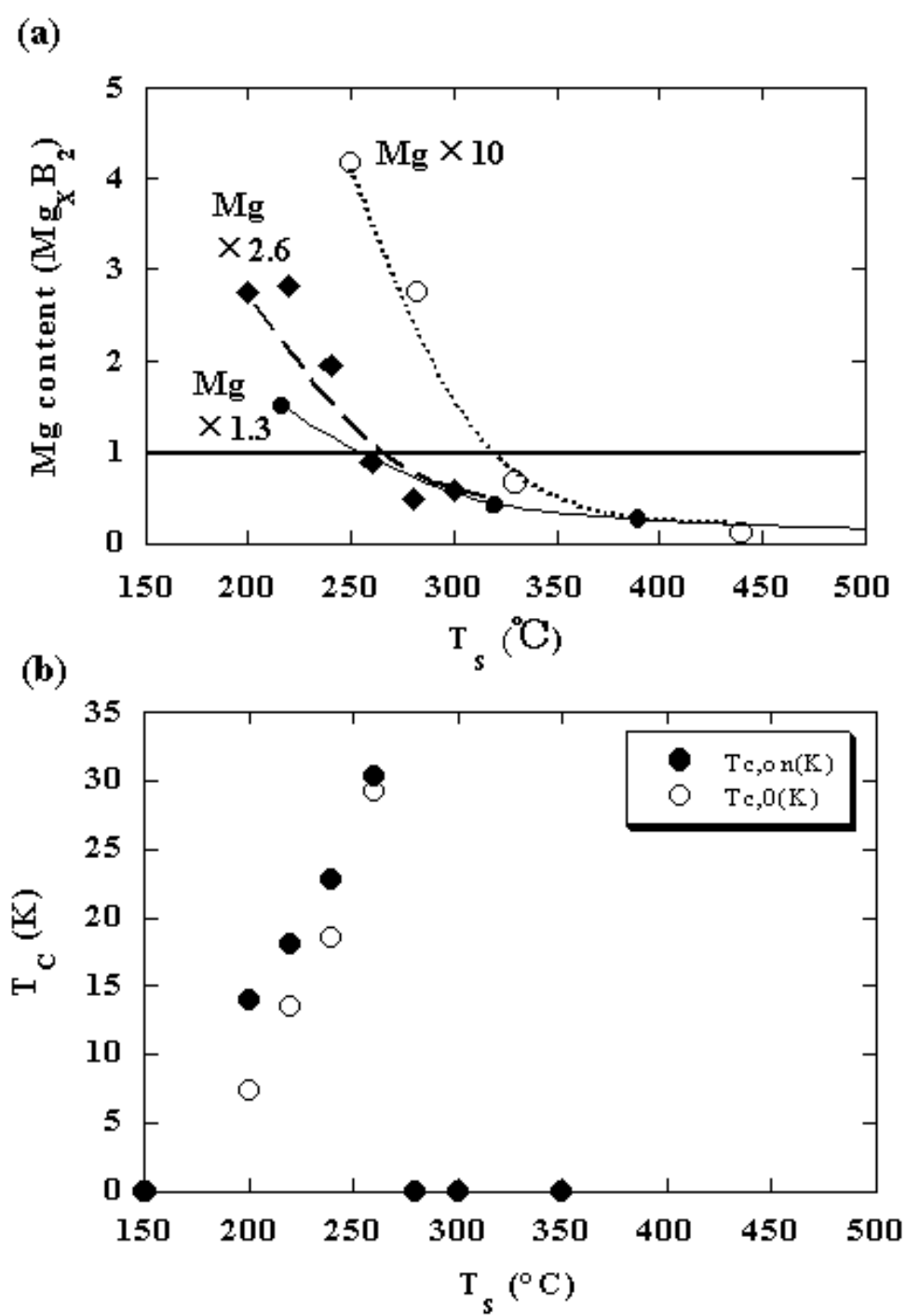


Fig. 2

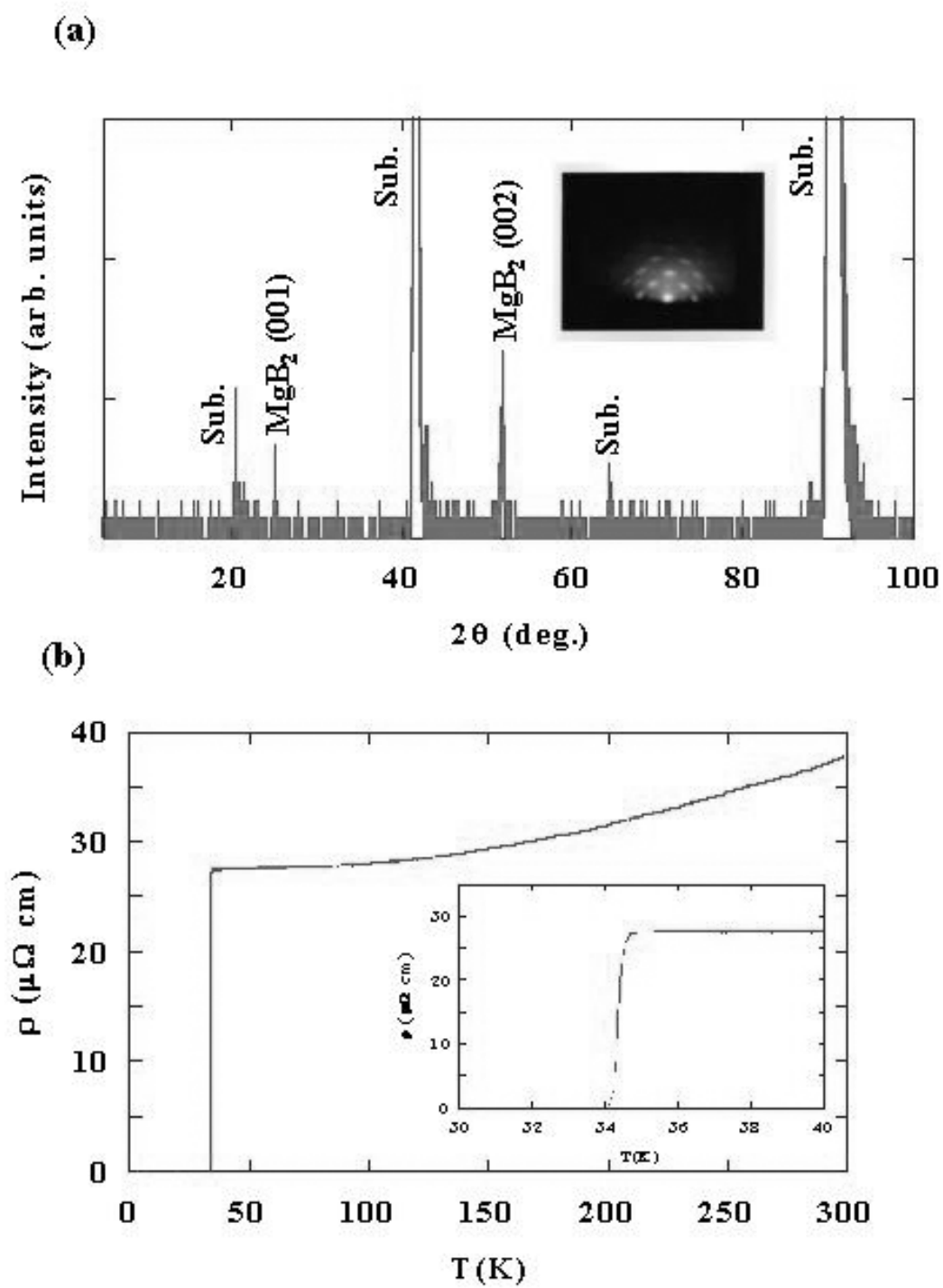


Fig. 3

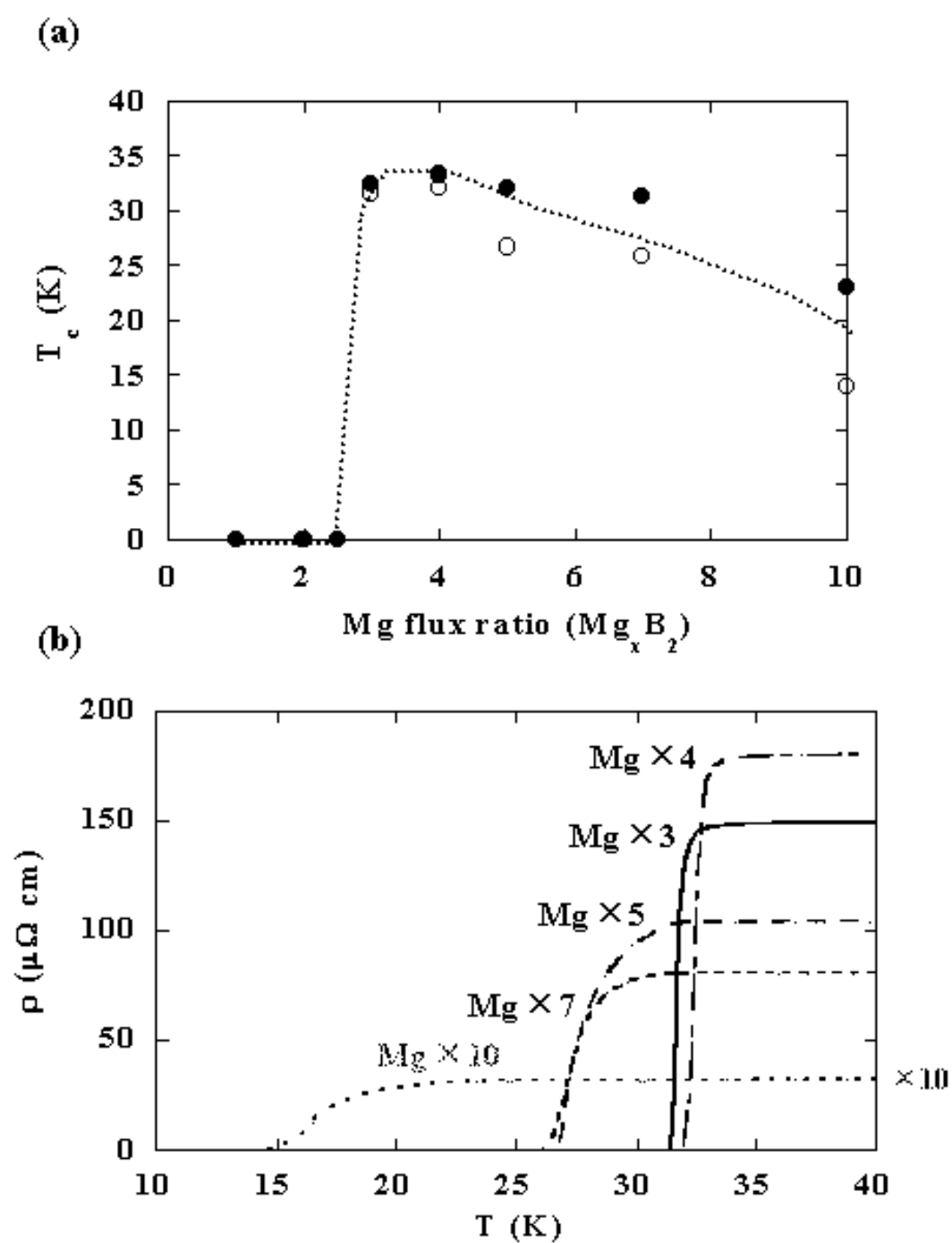


Fig. 4

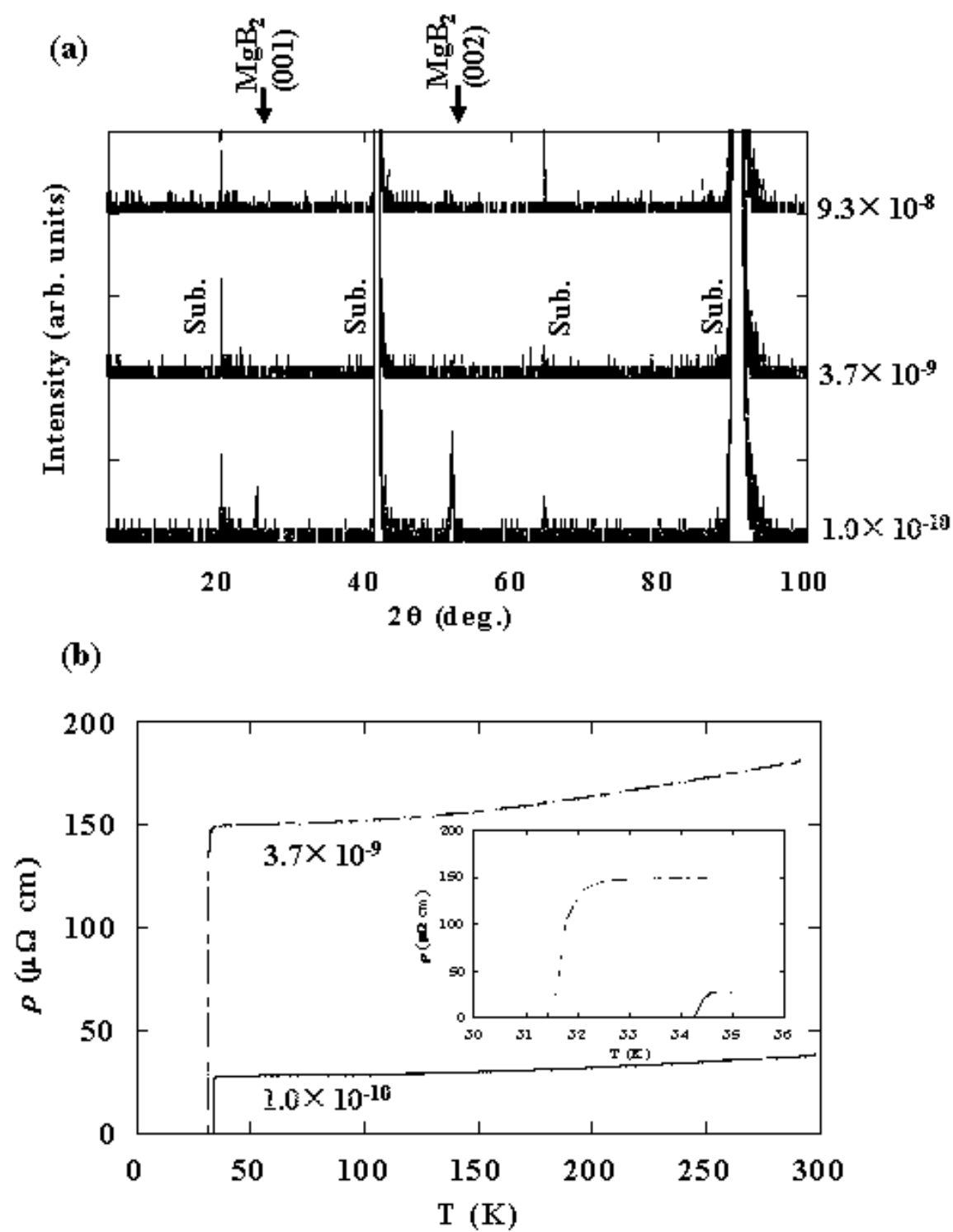


Fig. 5

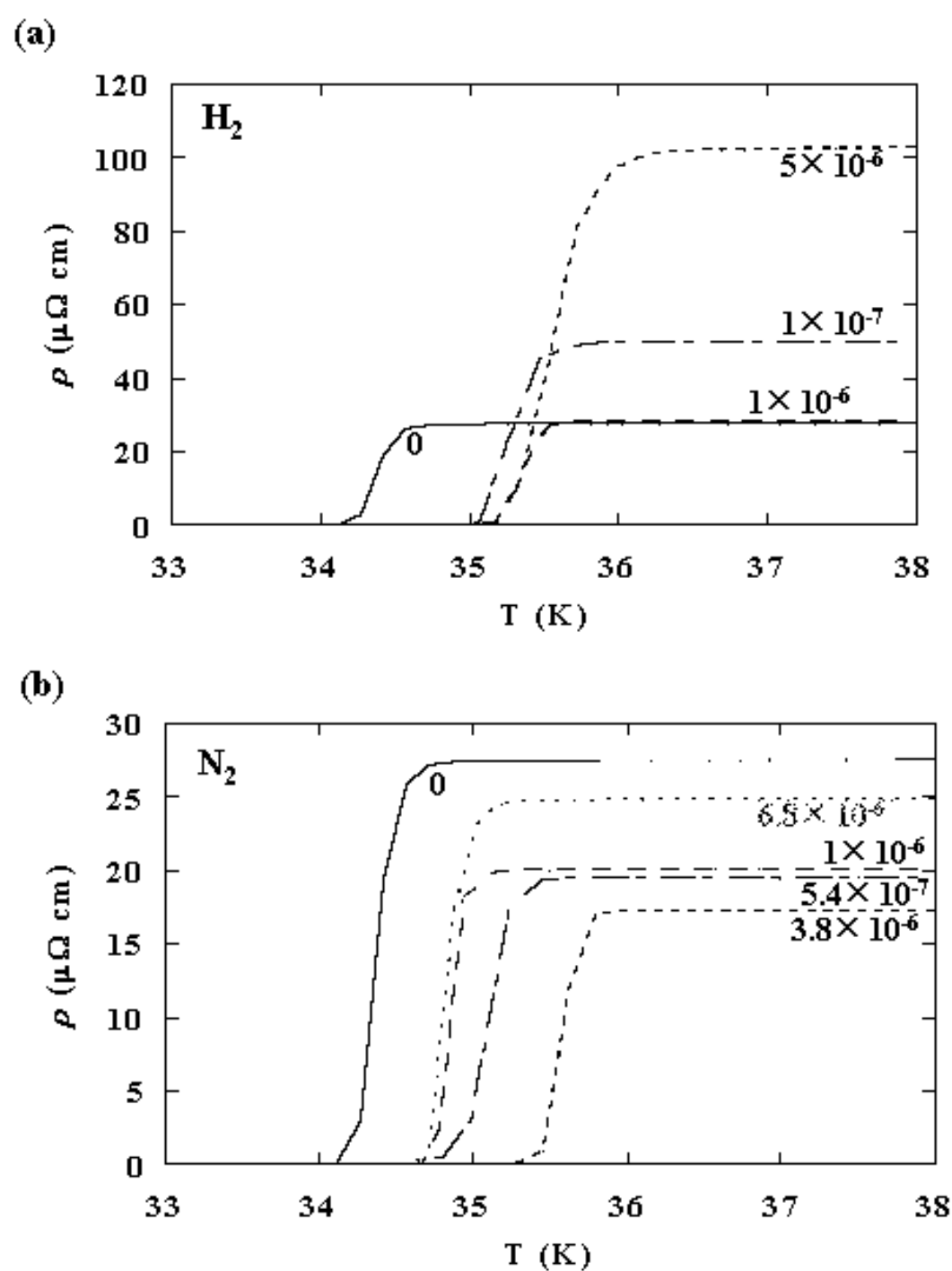


Fig. 6

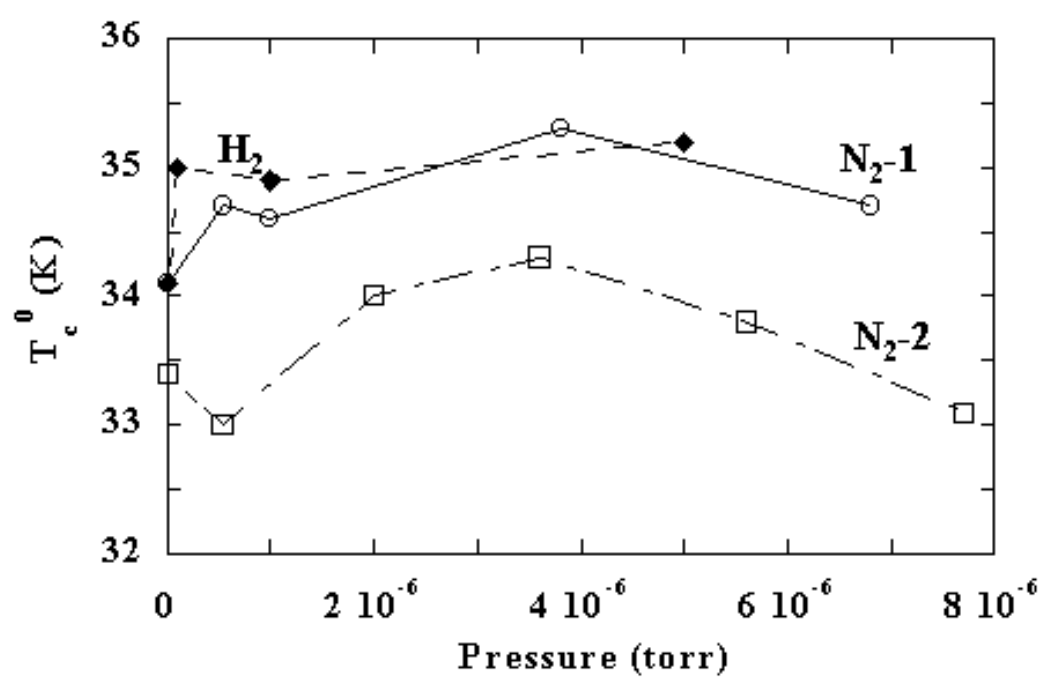


Fig. 7

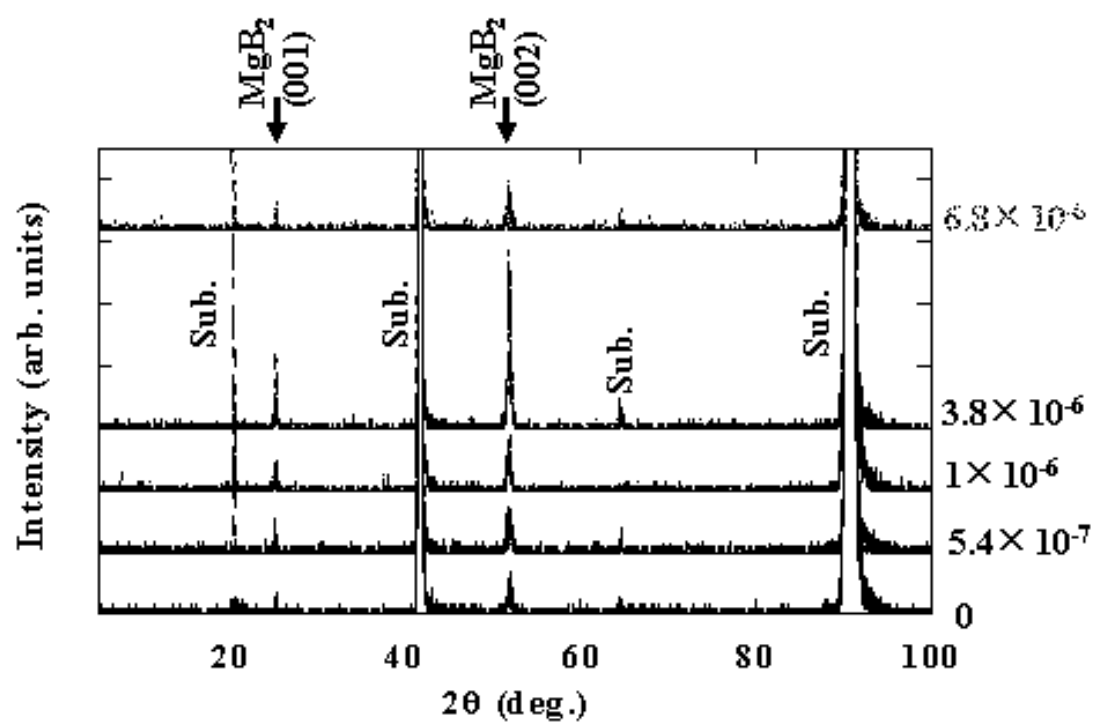


Fig. 8

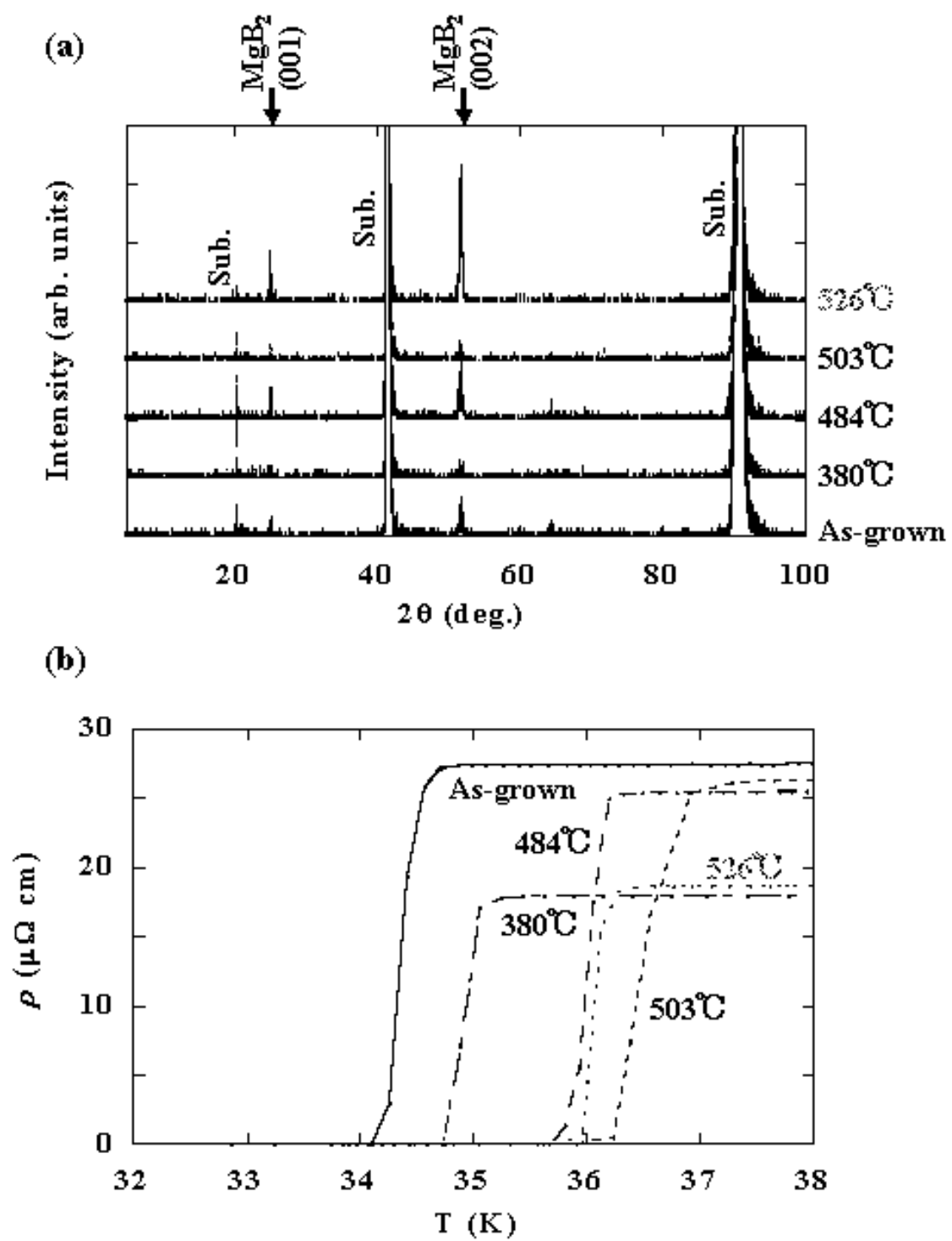


Fig. 9

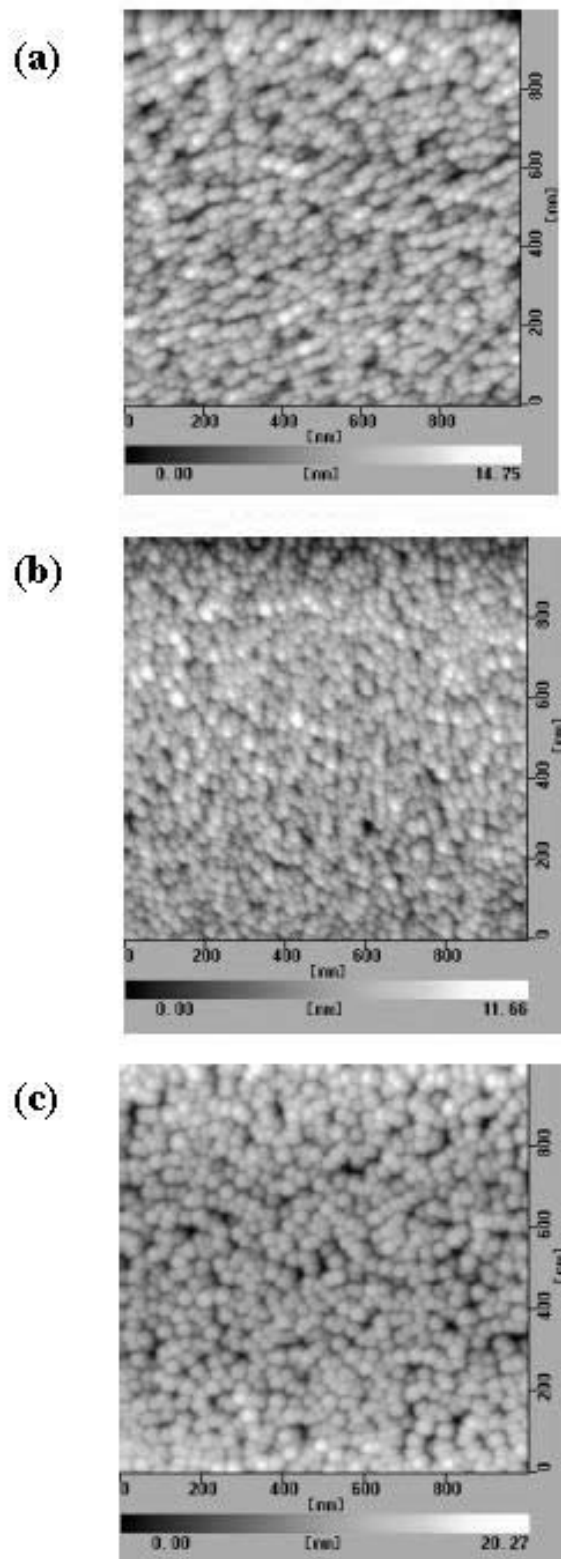


Fig. 10

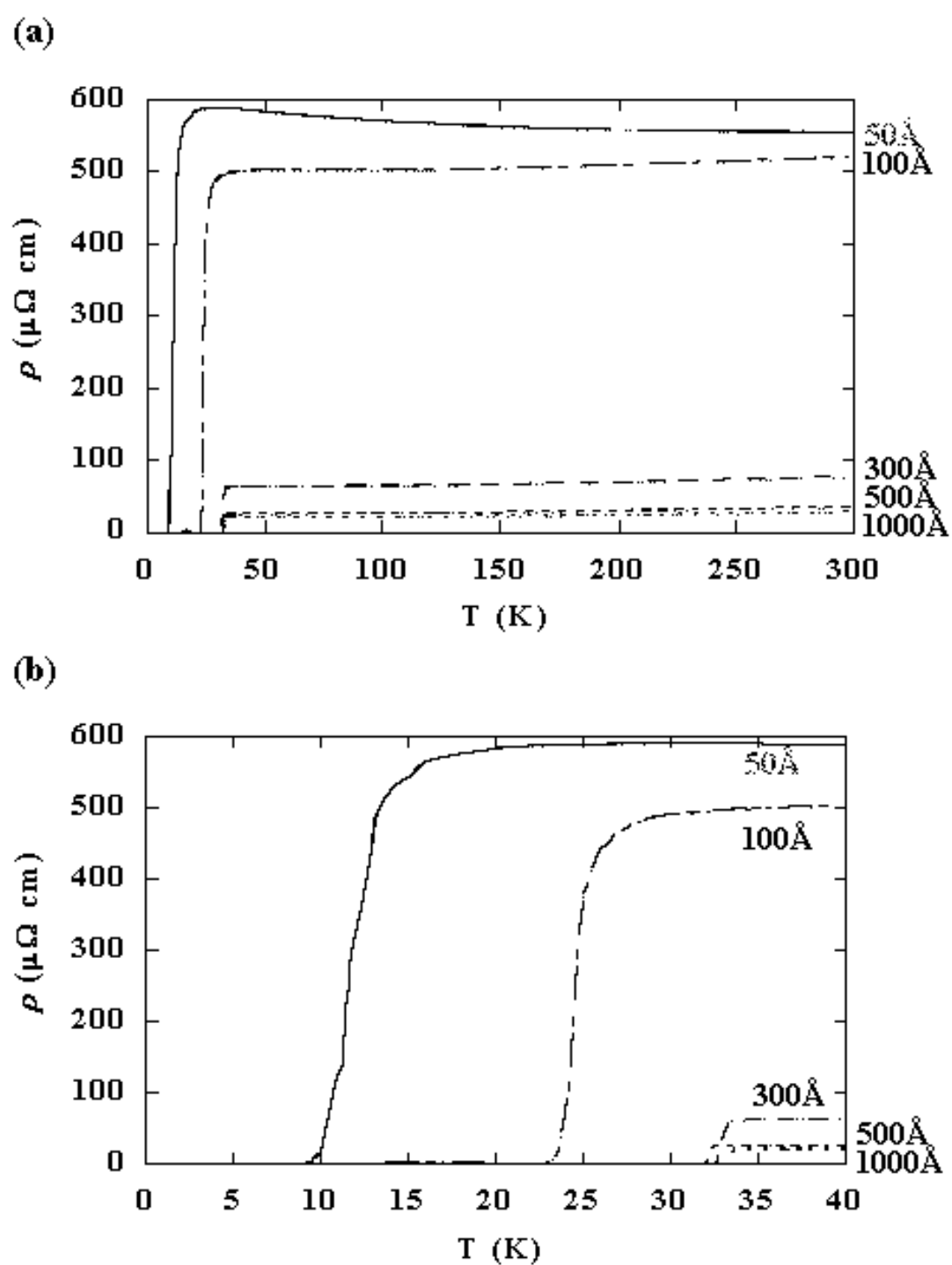


Fig. 11

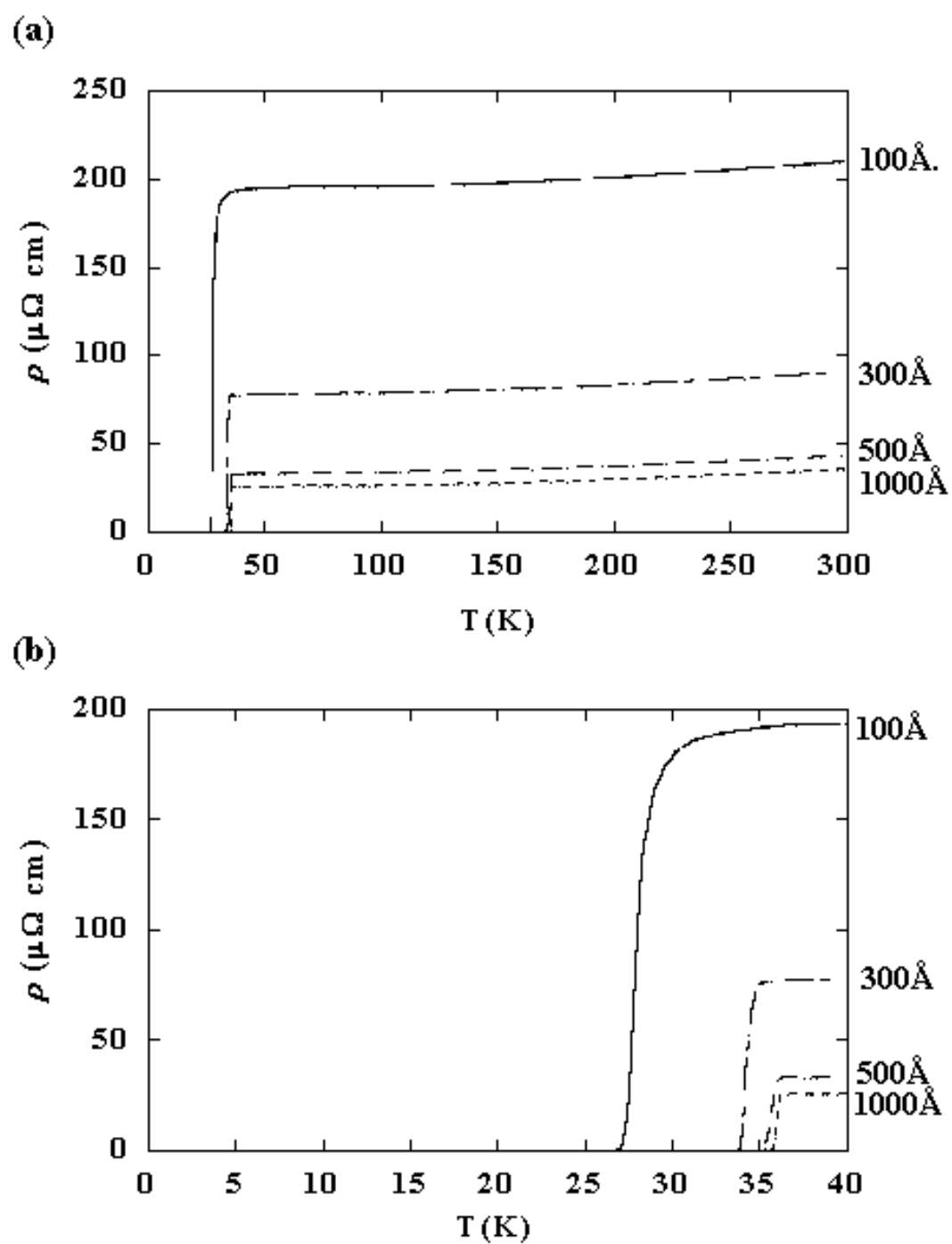


Fig. 12

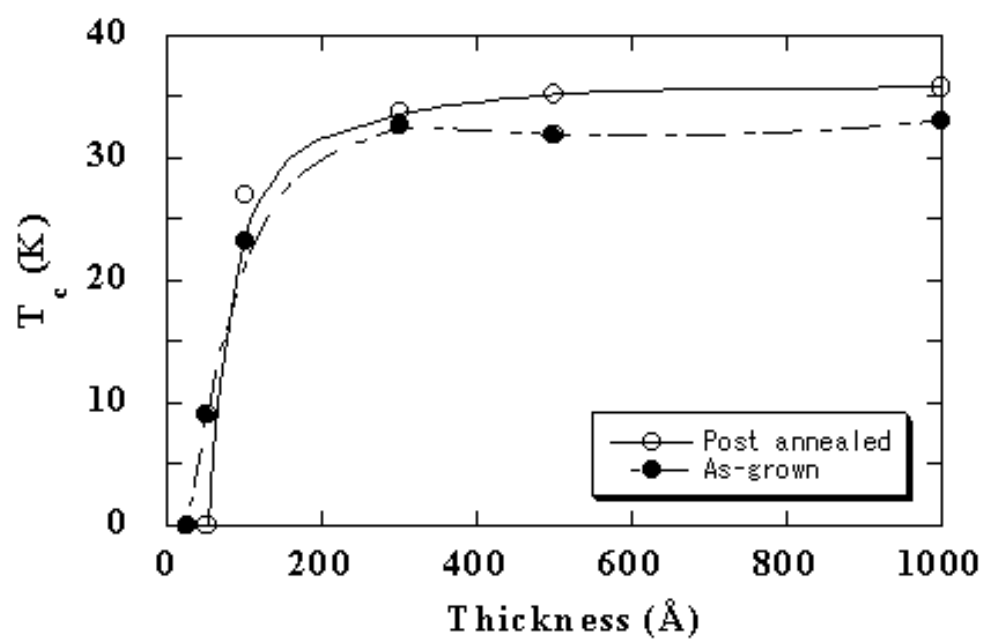


Fig. 13

(a)



(b)



Fig. 14

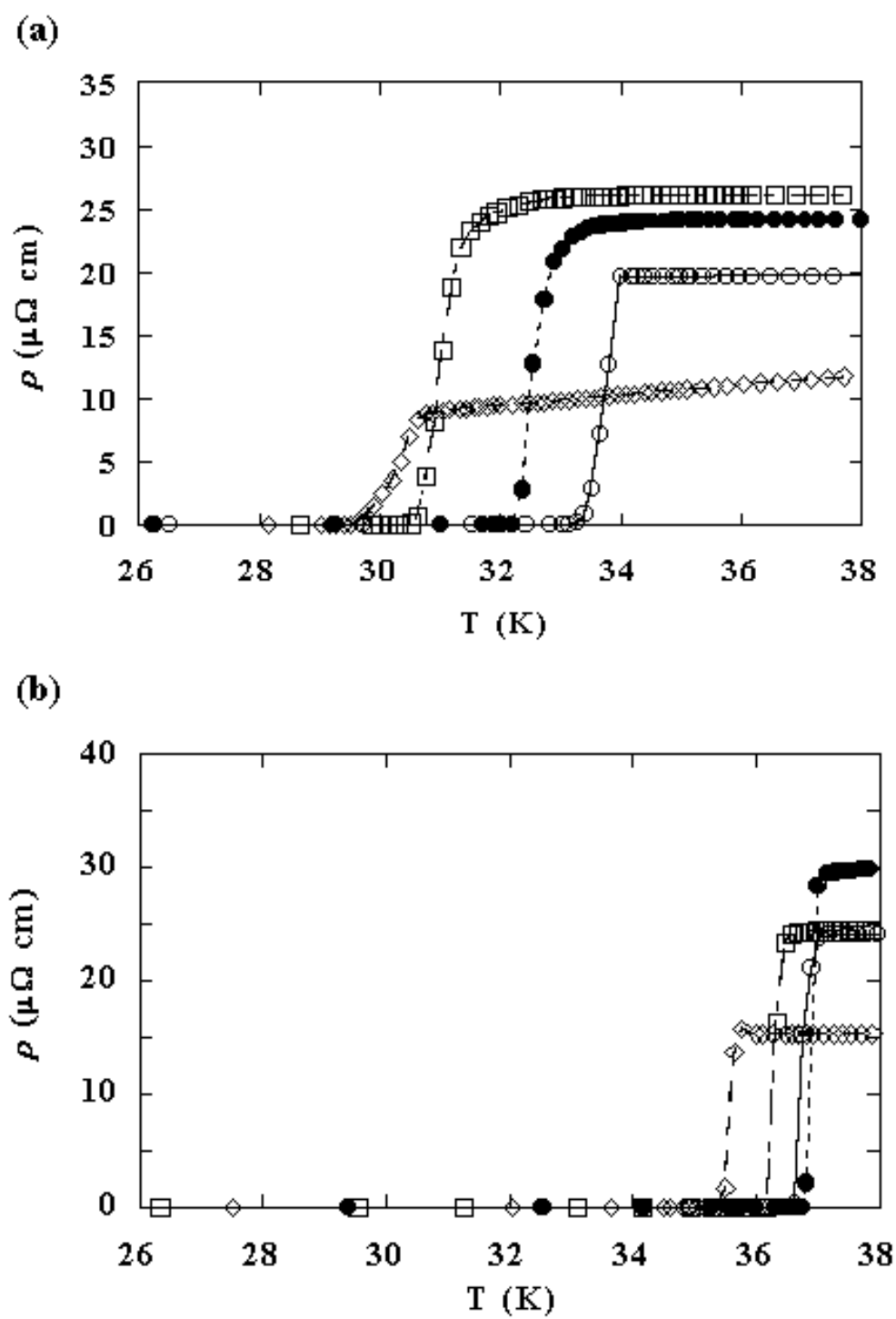


Fig. 15

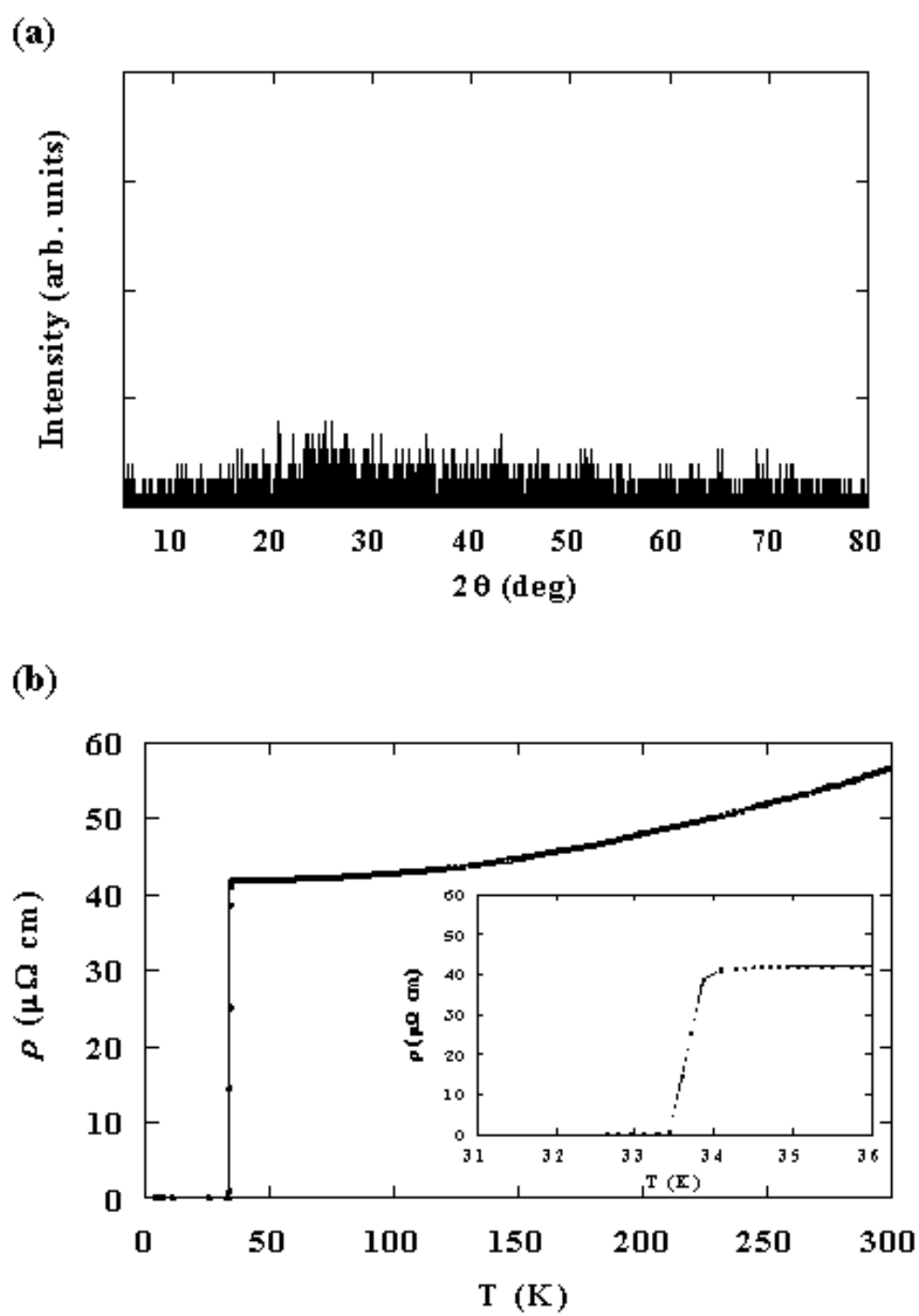


Fig. 16